Geology, published online on 19 March 2015 as doi:10.1130/G36467.1

Global increase in plant carbon isotope fractionation following the Last Glacial Maximum caused by increase in atmospheric pCO_2

Brian A. Schubert[1] and A. Hope Jahren[2]
[1]School of Geosciences, University of Louisiana at Lafayette, Lafayette, Louisiana 70504, USA
[2]SOEST (School of Ocean and Earth Science and Technology), University of Hawaii at Mānoa, Honolulu, Hawaii 96822, USA

ABSTRACT

Changes in the carbon isotope composition of terrestrial plant tissue ($\delta^{13}C$) are widely cited for evidence of shifts in climate, vegetation, or atmospheric chemistry across a wide range of time scales. A global compilation of $\delta^{13}C$ data from fossil leaves and bulk terrestrial organic matter (TOM) spanning the past 30 k.y., however, shows wide variability and no discernable trend. Here we analyze these data in terms of a relative change in net carbon isotope fractionation between the $\delta^{13}C$ value of plant tissue and that of atmospheric CO_2 [$\Delta^{13}C = (\delta^{13}C_{CO_2} - \delta^{13}C)/(1 + \delta^{13}C/1000)$] and identify a global 2.1‰ shift in leaf and TOM $\Delta^{13}C$ that is synchronous with a global rise in pCO_2 documented from ice core data. We apply a relationship describing the effect of pCO_2 on $\Delta^{13}C$ to the global record of $\Delta^{13}C$ change documented here to reconstruct pCO_2 levels across the past 30 k.y. Our reconstructed pCO_2 levels are in excellent agreement with the ice core data and underscore the potential of the global terrestrial $\delta^{13}C$ record to serve as an accurate pCO_2 proxy.

INTRODUCTION

Changes in the carbon stable isotope composition of terrestrial plant-derived substrates ($\delta^{13}C$) have been observed in the geological record at both local and global scales (e.g., McInerney and Wing, 2011). Such changes have been variously interpreted to record a change in environmental variables, including plant species composition (e.g., Feakins et al., 2013; Tipple and Pagani, 2010), water availability (e.g., Stewart et al., 1995), atmospheric oxygen concentration (Tappert et al., 2013), the isotopic composition of CO_2 in the atmosphere ($\delta^{13}C_{CO_2}$) (e.g., Jahren et al., 2001), and atmospheric pCO_2 (e.g., Schubert and Jahren, 2013). Changes within an isotope record from a single locality may reflect changes in local climate and vegetation, and so multiple high-resolution records from diverse environments are necessary to analyze for changes in global climate. The Quaternary Period is particularly rich in terrestrial $\delta^{13}C$ records, as well as in high-precision environmental data (e.g., $\delta^{13}C_{CO_2}$, pCO_2) from ice cores. We compile the global record of C_3 plant-derived $\delta^{13}C$ values from the Late Glacial through the Holocene and quantify changes in the carbon isotope fractionation between the atmosphere and plant-derived substrates through time. We build upon our previous work (Schubert and Jahren, 2012) that quantified the dependence of carbon isotope fractionation on pCO_2 during photosynthesis, based on observations during plant growth experiments. Here we apply this relationship to the global record of bulk terrestrial organic matter (TOM) and plant leaf fossil $\delta^{13}C$ in order to reconstruct changes in atmospheric pCO_2 across the past 30 k.y. We then compare our reconstruction to the values of pCO_2 known from ice cores, thus evaluating the potential of the original relationship to serve as an accurate proxy for paleo-pCO_2.

METHODS

In order to examine the global plant $\delta^{13}C$ record for the past 30 k.y., we compiled $\delta^{13}C$ values of fossil leaves and bulk TOM (includes bulk organic carbon measured in sediments, soil organic matter, loess, and peat deposits) from records that spanned at least 5 k.y. or extended from the Holocene to at least part of the glacial-interglacial transition (Termination 1; 18,000–11,500 yr before A.D. 1950, herein yr ago). Because we sought records of C_3 land plant carbon in equilibrium with a well-mixed atmosphere, we only compiled records that contained $\delta^{13}C$ values between −18.5‰ and −32‰ (after Kohn, 2010; O'Leary, 1988). We therefore avoided records with $\delta^{13}C$ values representative of C_4 plants (e.g., Pendall et al., 1999) or understory vegetation within closed canopy forests (e.g., Giresse et al., 1994), and records with bulk organic matter that contained significant inputs from aquatic plants or planktonic algae (e.g., Ji et al., 2005). The resulting data set yielded a total of 614 $\delta^{13}C$ measurements from 23 distinct records reported in 19 published studies (Table DR1 and Fig. DR1 in the GSA Data Repository[1]), and represents a wide range of values, similar to that observed for modern studies of whole leaves (Kohn, 2010) and integrated C_3 ecosystems (Pataki et al., 2003); leaf tissue ranged from −20.80‰ to −30.00‰ and TOM ranged from −18.50‰ to −31.75‰ (Fig. 1A).

In order to eliminate the effects of changes in the $\delta^{13}C$ value of atmospheric CO_2 ($\delta^{13}C_{CO_2}$) on the $\delta^{13}C$ value of plant tissue, we calculated the net carbon isotope fractionation [$\Delta^{13}C = (\delta^{13}C_{CO_2} - \delta^{13}C) / (1 + \delta^{13}C/1000)$; Farquhar et al., 1989] for each data point using $\delta^{13}C_{CO_2}$ values obtained from high-resolution ice core data (Elsig et al., 2009; Lourantou et al., 2010; Smith et al., 1999) (Fig. DR2; Table DR1). Because the absolute $\Delta^{13}C$ value is known to differ among plants growing under the same environmental conditions (e.g., Flanagan et al., 1997; Leavitt and Newberry, 1992), we analyzed the data set in terms of a relative change in the $\Delta^{13}C$ value between some time, t, and a reference time ($t = 0$), designated here as $\Delta(\Delta^{13}C)$:

$$\Delta(\Delta^{13}C) = \Delta^{13}C_{(t)} - \Delta^{13}C_{(t=0)}. \quad (1)$$

Figure 1B shows $\Delta(\Delta^{13}C)$ calculated using Equation 1 for all the isotope records compiled in Figure 1A (for an analysis of error, see the Data Repository). Within Equation 1, values for $\Delta^{13}C_{(t=0)}$ were calculated using the average Holocene $\delta^{13}C$ value for each record (listed in Table DR1) and $\delta^{13}C_{CO_2}$ was set equal to the average Holocene $\delta^{13}C_{CO_2}$ value (−6.4‰) calculated from the ice core record (Lüthi et al., 2008). Values for $\Delta^{13}C_{(t)}$ were calculated using the $\delta^{13}C$ data plotted in Figure 1A and $\delta^{13}C_{CO_2}$ values obtained from ice core data (Fig. DR2). We used ages reported in the original publications for all data. When calendar ages were not reported in a published paper, radiocarbon ages were converted to calendar ages using the radiocarbon calibration program described by Fairbanks et al. (2005).

RESULTS AND DISCUSSION

We identify a global 2.1‰ increase in $\Delta(\Delta^{13}C)$ measured in both fossil leaves and TOM (Fig. 1B) that is not apparent within the wide range of absolute $\delta^{13}C$ values shown within Figure 1A. We here explain this global 2.1‰ increase in $\Delta(\Delta^{13}C)$ by considering the effect of pCO_2 on carbon isotope fractionation and noting the 80 ppmv rise in pCO_2 documented across this interval from ice core data (Fig. 1C). We previously demonstrated that change in $\Delta^{13}C$ per unit increase in pCO_2 follows a continuous function (Schubert and Jahren, 2012) and updated this work with published data on 17 additional species including trees, shrubs, and herbaceous plants, and for both angiosperm and gymnosperm taxa (Table DR2). Taken together,

[1]GSA Data Repository item 2015151, all data presented in Figures 1 and 2, and a description of the errors associated with our reconstructed pCO_2 levels, is available online at www.geosociety.org/pubs/ft2015.htm, or on request from editing@geosociety.org or Documents Secretary, GSA, P.O. Box 9140, Boulder, CO 80301, USA.

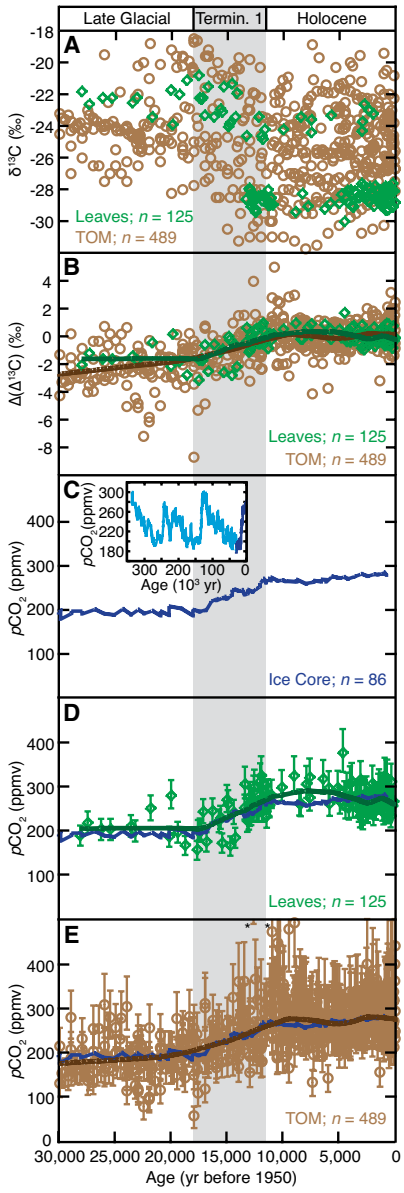

Figure 1. Carbon isotope values and pCO_2 levels across the past 30 k.y. A: $\delta^{13}C$ values from leaves (n = 125) and terrestrial organic matter (TOM; n = 489) compiled from 23 published records and used to calculate $\Delta(\Delta^{13}C)$. B: $\Delta(\Delta^{13}C)$ (Equation 1). C: pCO_2 levels from ice core records (Kawamura et al., 2007; Petit et al., 1999) (also plotted in D and E). D: pCO_2 levels through time reconstructed for leaves using Equation 4 and the $\Delta(\Delta^{13}C)$ data in B. E: pCO_2 levels through time reconstructed for TOM. Heavy curves in B, D, and E are locally weighted regression curves (loess, α = 0.25). Error bars in D and E indicate maximum cumulative error in the reconstructed pCO_2 values based upon the precision associated with determination of $\Delta(\Delta^{13}C)$ and $pCO_{2(t\ =\ 0)}$, and constants A, B, and C in Equation 4 (for error analysis, see the Data Repository [see footnote 1]). Reconstructed pCO_2 levels >500 ppmv (n = 2) are marked with asterisks. The interval of pCO_2 change (18,000–11,500 yr ago) across Termination 1 (Termin. 1) is shaded gray. A complete list of all isotope data and calculated pCO_2 values and their errors are provided in Table DR1 (see footnote 1).

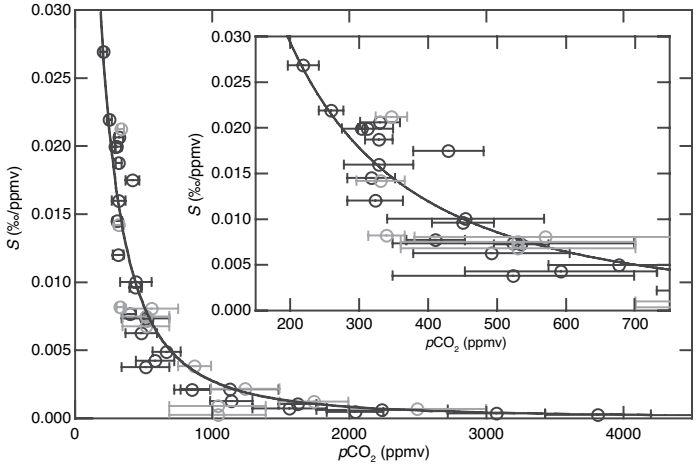

Figure 2. The effect of pCO_2 on C_3 land plant carbon isotope fractionation. Across field and chamber experiments on a wide range of C_3 land plant species, the amount of carbon isotope fractionation per change in pCO_2 (S, ‰/ppmv) decreases within increasing pCO_2 level according to Equation 2 (where A = 28.26, B = 0.22, and C = 23.9; r = 0.94; n = 40; black curve). Horizontal bars encompass the range of pCO_2 levels used within each experiment; the circle is plotted at the midpoint of the range. Inset shows the data plotted across pCO_2 = 150–750 ppmv. We updated the original data set (Schubert and Jahren, 2012) (black circles, n = 28) with additional published data (gray circles, n = 12). All values and references are provided in Table DR2 (see footnote 1).

the data show that changes in $\Delta^{13}C$ per unit increase in pCO_2 (S, ‰/ppmv) decrease with increasing pCO_2 level according to the following general equation (r = 0.94, n = 40) (Fig. 2):

$$S = (A^2)(B) / [A + (B)(pCO_2 + C)]^2. \quad (2)$$

Integration of Equation 2 yields the following generalized hyperbolic relationship between $\Delta^{13}C$ and pCO_2:

$$\Delta^{13}C = [(A)(B)(pCO_2 + C)] / [A + (B)(pCO_2 + C)], \quad (3)$$

where A = 28.26, B = 0.22, and C = 23.9. The values for A, B, and C were determined iteratively such that $\Delta^{13}C$ = 4.4‰ at pCO_2 = 0 ppmv, and $\Delta^{13}C$ = 28.26‰ at $pCO_2 = 10^6$ ppmv (after Schubert and Jahren, 2012). The change in $\Delta^{13}C$ [$\Delta(\Delta^{13}C)$, Equation 1] that results from a change in pCO_2 can then be described by the following equation (after Equation 3 and Schubert and Jahren, 2013):

$$\Delta(\Delta^{13}C) = [(A)(B)(pCO_{2(t)} + C)] / [A + (B)(pCO_{2(t)} + C)] - [(A)(B)(pCO_{2(t\ =\ 0)} + C)] / [A + (B)(pCO_{2(t\ =\ 0)} + C)]. \quad (4)$$

We can therefore use $\Delta(\Delta^{13}C)$ data to solve for pCO_2 at any time t ($pCO_{2(t)}$), provided we know the pCO_2 level at reference time t = 0 (i.e., $pCO_{2(t\ =\ 0)}$); values for A, B, and C are the same as in Equation 3.

We reconstructed pCO_2 levels for the past 30 k.y. using Equation 4 with $pCO_{2(t\ =\ 0)}$ = 270 ppmv (the average preindustrial Holocene level; Kawamura et al., 2007) and the $\Delta(\Delta^{13}C)$ data shown in Figure 1B. The result shows excellent agreement with pCO_2 levels obtained from high-resolution ice core data spanning the past 30 k.y. (Figs. 1D and 1E). Both the fossil leaf and TOM records indicate a steady increase in pCO_2 across Termination 1 (18,000–11,500 yr ago) with little change in pCO_2 during the Holocene (11,500–100 yr ago) and the Late Glacial interval (30,000–18,000 yr ago), corroborated by the ice core record both with respect to trends as well as absolute values (Table 1). Across the entire record, the average absolute difference between the pCO_2 level determined from the ice core and the $pCO_{2(t)}$ level reconstructed using Equation 4 is small (23 and 39 ppmv for fossil leaves and TOM, respectively) and the correlations between the ice core record and the locally weighted regression (loess, α = 0.25) through each substrate are high (R^2 = 0.97 and R^2 = 0.80 for TOM and fossil leaves, respectively).

TABLE 1. COMPARISON OF pCO_2 LEVELS DETERMINED FOR SPECIFIC INTERVALS USING LEAF AND TERRESTRIAL ORGANIC MATTER (EQUATION 4) WITH HIGH-RESOLUTION ICE CORE DATA

Interval* (yr ago)	Ice core**	Leaves	TOM††
Holocene† 11,499–100	270 ± 7 ppmv (n = 38)	273 ± 27 ppmv (n = 76)	278 ± 52 ppmv (n = 281)
Termination 1§ 17,999–11,500	0.0102 ppmv/yr (n = 26)	0.0137 ppmv/yr (n = 38)	0.0096 ppmv/yr (n = 84)
Late Glacial† 30,000–18,000	193 ± 7 ppmv (n = 22)	209 ± 31 ppmv (n = 11)	188 ± 45 ppmv (n = 117)

*0 yr ago = A.D. 1950.
†Holocene and Late Glacial pCO_2 levels reported as mean ±1σ.
§Calculated as the slope of a best-fit line through the data spanning this interval.
**Ice core data calculated from Kawamura et al. (2007).
††TOM—terrestrial organic matter. Two values (marked with asterisks in Fig. 1E) were excluded from the calculations.

We note that all TOM and fossil leaf carbon isotope records are subject to variability arising from differential water availability, which has been shown to be a primary environmental driver of changes in $\delta^{13}C$ value, both in terms of mean annual precipitation (Diefendorf et al., 2010; Kohn, 2010) and seasonal precipitation (Schubert and Jahren, 2011). We examine the scatter about the mean for both $\Delta(\Delta^{13}C)$ records, calculated as the average absolute difference between the measured $\Delta(\Delta^{13}C)$ values (Equation 1) and the locally weighted regression curves (Fig. 1B). The scatter within both the TOM $\Delta(\Delta^{13}C)$ record (0.87‰ ± 0.82‰, n = 489) and the fossil leaf record (0.46‰ ± 0.38‰, n = 125) probably reflects the heterogeneous environmental influences (e.g., water availability) that cause $\delta^{13}C$ variability within and between ecosystems (reviewed by Dawson et al., 2002). The significantly ($p < 0.0001$) greater scatter within the TOM data set also reflects the changing contributions of different plant species and taxonomic groups, which are known to show different amounts of carbon isotope fractionation (Flanagan et al., 1997; Leavitt and Newberry, 1992). In contrast, the fossil leaf records are based on measurements across single species (e.g., *Pinus flexilis*; Van de Water et al., 1994); therefore, the variance within the fossil leaves data set (0.15) is 4.5× lower than the variance within the TOM data set (0.68), reflecting the reduced sources of isotopic variability within species-specific substrates. When we quantify the scatter in reconstructed pCO_2 values for each substrate, calculated as the absolute difference between $pCO_{2(t)}$ (calculated from Equation 4) and the locally weighted regression curve fit through the calculated $pCO_{2(t)}$ values, we find that for both fossil leaves and TOM this scatter is small; the average values (±1σ) are 21 ± 17 ppmv (n = 125) for fossil leaves and 39 ± 44 ppmv (n = 489) for TOM. Our analysis reinforces our claim that although local environmental factors influence plant $\delta^{13}C$ value, the governing influence of pCO_2 over carbon isotope fractionation is apparent within global data sets. We contend that global shifts in the amount of carbon isotope fractionation of C_3 terrestrial plant tissue are best interpreted to reflect a change in pCO_2 because a global record averages the effects of local or regional changes in environmental conditions, substrate heterogeneity, and plant community shifts.

Our results also illustrate how the effect of pCO_2 on changing plant carbon isotope composition, if not acknowledged, may lead to inappropriate paleoclimate interpretations. As an example, the combined leaf and TOM data set shows a global 2.1‰ relative increase in carbon isotope fractionation from the Late Glacial to the Holocene (Fig. 1B). If we hypothesize a Late Glacial mean annual precipitation (MAP) of 830 mm (the simulated Last Glacial Maximum MAP over land; Vettoretti et al., 2000) and apply the proposed relationship between MAP and $\Delta^{13}C$ values (Kohn, 2010, his equation 2), the 2.1‰ increase would require a 1442 mm increase to MAP = 2272 mm (i.e., ~3× greater than modern MAP), an extreme change not corroborated within the sedimentological, geochemical, or fossil records of the period. Similarly, there is no independent evidence across this interval that would support an interpretation of a global change in C_3 plant community composition. A significant rise in global temperatures coincided with the increases in pCO_2 level across Termination 1 (Parrenin et al., 2013), but the measured effect of an increase in temperature on plant carbon isotope fractionation varies (King et al., 2012; Schleser et al., 1999) and may be autocorrelated with changes in precipitation, cloudiness, and/or humidity (e.g., McCarroll and Pawellek, 2001). Moreover, the shift observed here is the opposite of what would be expected from an increase in global water stress due to a rise in global temperature across Termination 1. Thus, although climate change may affect the plant carbon isotope record of a single site, it cannot explain the global record presented here.

CONCLUSIONS

Our analysis reveals that the ~80 ppmv rise in pCO_2 level from the Late Glacial to preindustrial levels evident within air bubbles in glacial ice (Kawamura et al., 2007) is recorded by the global record of carbon isotope fractionation in C_3 land plants. Excellent agreement between our reconstructed levels and those measured from ice demonstrates the potential for using terrestrial carbon isotope records to reconstruct atmospheric pCO_2 for periods when any change in $\delta^{13}C_{CO_2}$ is independently constrained, either by the ice core record as illustrated here, or by the nonphotosynthetic marine record in the more distant past (Schubert and Jahren, 2013; Tipple et al., 2010). We warn that before interpreting environmental change from the $\delta^{13}C$ value of terrestrial substrates, the effect of changing pCO_2 levels must be considered, particularly for intervals with moderate to low pCO_2 levels that dominated much of the past 350 m.y. (Breecker et al., 2010; Franks et al., 2014). We note that changes in atmospheric oxygen concentrations (pO_2) may also prove to be important on these longer time scales (e.g., Beerling et al., 2002; Berner et al., 2000), but the systematic study of the effect of pO_2 in isolation from seed to maturity across the full range of pO_2 levels predicted for the geologic past is lacking. Changes in pCO_2 that result from changes in elevation also affect carbon isotope measurements (high-elevation plants show less fractionation than low-elevation plants and pCO_2 declines with increasing elevation; Körner et al., 1988), and therefore elevation changes should be considered when examining $\Delta^{13}C$ change on multimillion-year time scales. Independent of these effects, our work demonstrates the potential for terrestrial $\delta^{13}C$ measurements to be used for reconstructing pCO_2 levels in the geologic record.

ACKNOWLEDGMENTS

This material is based upon work supported by the U.S. Department of Energy, Office of Science, Office of Basic Energy Sciences, Chemical Sciences, Geosciences and Biosciences Division under awards DE-FG02-13ER16412 (Schubert) and DE-FG02-09ER16002 (Jahren).

REFERENCES CITED

Beerling, D.J., Lake, J.A., Berner, R.A., Hickey, L.J., Taylor, D.W., and Royer, D.L., 2002, Carbon isotope evidence implying high O_2/CO_2 ratios in the Permo-Carboniferous atmosphere: Geochimica et Cosmochimica Acta, v. 66, p. 3757–3767, doi:10.1016/S0016-7037(02)00901-8.

Berner, R.A., et al., 2000, Isotope fractionation and atmospheric oxygen: Implications for Phanerozoic O_2 evolution: Science, v. 287, p. 1630–1633, doi:10.1126/science.287.5458.1630.

Breecker, D.O., Sharp, Z.D., and McFadden, L.D., 2010, Atmospheric CO_2 concentration during ancient greenhouse climates were similar to those predicted for A.D. 2100: National Academy of Sciences Proceedings, v. 107, p. 576–580, doi:10.1073/pnas.0902323106.

Dawson, T.E., Mambelli, S., Plamboeck, A.H., Templer, P.H., and Tu, K.P., 2002, Stable isotopes in plant ecology: Annual Review of Ecology and Systematics, v. 33, p. 507–559, doi:10.1146/annurev.ecolsys.33.020602.095451.

Diefendorf, A.F., Mueller, K.E., Wing, S.L., Koch, P.L., and Freeman, K.H., 2010, Global patterns in leaf ^{13}C discrimination and implications for studies of past and future climate: National Academy of Sciences Proceedings, v. 107, p. 5738–5743, doi:10.1073/pnas.0910513107.

Elsig, J., Schmitt, J., Leuenberger, D., Schneider, R., Eyer, M., Leuenberger, M., Joos, F., Fischer, H., and Stocker, T.F., 2009, Stable isotope constraints on Holocene carbon cycle changes from an Antarctic ice core: Nature, v. 461, p. 507–510, doi:10.1038/nature08393.

Fairbanks, R.G., Mortlock, R.A., Chiu, T.-C., Cao, L., Kaplan, A., Guilderson, T.P., Fairbanks, T.W., Bloom, A.L., Grootes, P.M., and Nadeau, M.-J., 2005, Radiocarbon calibration curve spanning 0 to 50,000 years BP based on paired $^{230}Th/^{234}U/^{238}U$ and ^{14}C dates on pristine corals: Quaternary Science Reviews, v. 24, p. 1781–1796, doi:10.1016/j.quascirev.2005.04.007.

Farquhar, G.D., Ehleringer, J.R., and Hubick, K.T., 1989, Carbon isotope discrimination and photosynthesis: Annual Review of Plant Physiology and Plant Molecular Biology, v. 40, p. 503–537, doi:10.1146/annurev.pp.40.060189.002443.

Feakins, S.J., Levin, N.E., Liddy, H.M., Sieracki, A., Eglinton, T.I., and Bonnefille, R., 2013, Northeast African vegetation change over 12 m.y.: Geology, v. 41, p. 295–298, doi:10.1130/G33845.1.

Flanagan, L.B., Brooks, J.R., and Ehleringer, J.R., 1997, Photosynthesis and carbon isotope discrimination in boreal forest ecosystems: A comparison of functional characteristics in plants from three mature forest types: Journal of Geophysical Research, v. 102, p. 28,861–28,869, doi:10.1029/97JD01235.

Franks, P.J., Royer, D.L., Beerling, D.J., Van de Water, P.K., Cantrill, D.J., Barbour, M.M., and Berry, J.A., 2014, New constraints on atmospheric CO_2 concentration for the Phanerozoic: Geophysical Research Letters, v. 41, p. 4685–4694, doi:10.1002/2014GL060457.

Giresse, P., Maley, J., and Brenac, P., 1994, Late Quaternary palaeoenvironments in the Lake Barombi Mbo (west Cameroon) deduced from pollen and carbon isotopes of organic matter: Palaeogeography, Palaeoclimatology, Palaeoecology, v. 107, p. 65–78, doi:10.1016/0031-0182(94)90165-1.

Jahren, A.H., Arens, N.C., Sarmiento, G., Guerrero, J., and Amundson, R., 2001, Terrestrial record of methane hydrate dissociation in the Early Cretaceous: Geology, v. 29, p. 159–162, doi:10.1130/0091-7613(2001)029<0159:TRO MHD>2.0.CO;2.

Ji, S., Xingqi, L., Sumin, W., and Matsumoto, R., 2005, Palaeoclimatic changes in the Qinghai Lake area during the last 18,000 years: Quaternary International, v. 136, p. 131–140, doi:10.1016/j.quaint.2004.11.014.

Kawamura, K., Nakazawa, T., Aoki, S., Sugawara, S., Fujii, Y., and Watanabe, O., 2007, Dome Fuji ice core 338KYr wet extraction CO_2 data, *in* International Geosphere-Biosphere Programme PAGES/World Data Center for Paleoclimatology Data Contribution Series 2007-074: Boulder Colorado, National Oceanic and Atmospheric Administration National Climatic Data Center Paleoclimatology Program.

King, D.C., Schubert, B.A., and Jahren, A.H., 2012, Practical considerations for the use of pollen $\delta^{13}C$ value as a paleoclimate indicator: Rapid Communications in Mass Spectrometry, v. 26, p. 2165–2172, doi:10.1002/rcm.6333.

Kohn, M.J., 2010, Carbon isotope compositions of terrestrial C3 plants as indicators of (paleo)ecology and (paleo)climate: National Academy of Sciences Proceedings, v. 107, p. 19691–19695, doi:10.1073/pnas.1004933107.

Körner, C., Farquhar, G.D., and Roksandic, Z., 1988, A global survey of carbon isotope discrimination in plants from high altitude: Oecologia, v. 74, p. 623–632, doi:10.1007/BF00380063.

Leavitt, S.W., and Newberry, T., 1992, Systematics of stable-carbon isotopic differences between gymnosperm and angiosperm trees: Plant Physiology, v. 11, p. 257–262.

Lourantou, A., Lavrič, J.V., Köhler, P., Barnola, J.-M., Paillard, D., Michel, E., Raynaud, D., and Chappellaz, J., 2010, Constraint of the CO_2 rise by new atmospheric carbon isotopic measurements during the last deglaciation: Global Biogeochemical Cycles, v. 24, GB2015, doi:10.1029/2009GB003545.

Lüthi, D., et al., 2008, High-resolution carbon dioxide concentration record 650,000–800,000 years before present: Nature, v. 453, p. 379–382, doi:10.1038/nature06949.

McCarroll, D., and Pawellek, F., 2001, Stable carbon isotope ratios of *Pinus sylvestris* from northern Finland and the potential for extracting a climate signal from long Fennoscandian chronologies: The Holocene, v. 11, p. 517–526, doi:10.1191/095968301680223477.

McInerney, F.A., and Wing, S.L., 2011, The Paleocene–Eocene thermal maximum: A perturbation of carbon cycle, climate, and biosphere with implications for the future: Annual Review of Earth and Planetary Sciences, v. 39, p. 489–516, doi:10.1146/annurev-earth-040610-133431.

O'Leary, M.H., 1988, Carbon isotopes in photosynthesis: Bioscience, v. 38, p. 328–336, doi:10.2307/1310735.

Parrenin, F., Masson-Delmotte, V., Köhler, P., Raynaud, D., Paillard, D., Schwander, J., Barbante, C., Landais, A., Wegner, A., and Jouzel, J., 2013, Synochronous change of atmospheric CO_2 and Antarctic temperature during the last deglacial warming: Science, v. 339, p. 1060–1063, doi:10.1126/science.1226368.

Pataki, D.E., Ehleringer, J.R., Flanagan, L.B., Yakir, D., Bowling, D.R., Still, C.J., Buchmann, N., Kaplan, J.O., and Berry, J.A., 2003, The application and interpretation of Keeling plots in terrestrial carbon cycle research: Global Biogeochemical Cycles, v. 17, 1022, doi:10.1029/2001GB001850.

Pendall, E., Betancourt, J.L., and Leavitt, S.W., 1999, Paleoclimatic significance of δD and $\delta^{13}C$ values in piñon pine needles from packrat middens spanning the last 40,000 years: Palaeogeography, Palaeoclimatology, Palaeoecology, v. 147, p. 53–72, doi:10.1016/S0031-0182(98)00152-7.

Petit, J.R., et al., 1999, Climate and atmospheric history of the past 420,000 years from the Vostok ice core, Antarctica: Nature, v. 399, p. 429–436, doi:10.1038/20859.

Schleser, G.H., Helle, G., Lücke, A., and Vos, H., 1999, Isotope signals as climate proxies: The role of transfer functions in the study of terrestrial archives: Quaternary Science Reviews, v. 18, p. 927–943, doi:10.1016/S0277-3791(99)00006-2.

Schubert, B.A., and Jahren, A.H., 2011, Quantifying seasonal precipitation using high-resolution carbon isotope analyses in evergreen wood: Geochimica et Cosmochimica Acta, v. 75, p. 7291–7303, doi:10.1016/j.gca.2011.7208.7002.

Schubert, B.A., and Jahren, A.H., 2012, The effect of atmospheric CO_2 concentration on carbon isotope fractionation in C_3 land plants: Geochimica et Cosmochimica Acta, v. 96, p. 29–43, doi:10.1016/j.gca.2012.08.003.

Schubert, B.A., and Jahren, A.H., 2013, Reconciliation of marine and terrestrial carbon isotope excursions based on changing atmospheric CO_2 levels: Nature Communications, v. 4, 1653, doi:10.1038/ncomms2659.

Smith, H.J., Fischer, H., Wahlen, M., Mastroianni, D., and Deck, B., 1999, Dual modes of the carbon cycle since the Last Glacial Maximum: Nature, v. 400, p. 248–250, doi:10.1038/22291.

Stewart, G.R., Turnbull, M.H., Schmidt, S., and Erskine, P.D., 1995, ^{13}C natural abundance in plant communities along a rainfall gradient: A biological integrator of water availability: Australian Journal of Plant Physiology, v. 22, p. 51–55, doi:10.1071/PP9950051.

Tappert, R., McKellar, R.C., Wolfe, A.P., Tappert, M.C., Ortega-Blanco, J., and Muehlenbachs, K., 2013, Stable carbon isotopes of C3 plant resins and ambers record changes in atmospheric oxygen since the Triassic: Geochimica et Cosmochimica Acta, v. 121, p. 240–262, doi:10.1016/j.gca.2013.07.011.

Tipple, B.J., and Pagani, M., 2010, A 35 Myr North American leaf-wax compound-specific carbon and hydrogen isotope record: Implications for C_4 grasslands and hydrologic cycle dynamics: Earth and Planetary Science Letters, v. 299, p. 250–262, doi:10.1016/j.epsl.2010.09.006.

Tipple, B.J., Meyers, S.R., and Pagani, M., 2010, Carbon isotope ratio of Cenozoic CO_2: A comparative evaluation of available geochemical proxies: Paleoceanography, v. 25, PA3202, doi:10.1029/2009PA001851.

Van de Water, P.K., Leavitt, S.W., and Betancourt, J.L., 1994, Trends in stomatal density and $^{13}C/^{12}C$ ratios of *Pinus flexilis* needles during last glacial-interglacial cycle: Science, v. 264, p. 239–243, doi:10.1126/science.264.5156.239.

Vettoretti, G., Peltier, W.R., and McFarlane, N.A., 2000, Global water balance and atmospheric water vapour transport at last glacial maximum: Climate simulations with the Canadian Climate Centre for Modelling and Analysis atmospheric general circulation model: Canadian Journal of Earth Sciences, v. 37, p. 695–723, doi:10.1139/e99-092.

Manuscript received 19 November 2014
Revised manuscript received 13 February 2015
Manuscript accepted 22 February 2015

Printed in USA

Geology, published online on 19 March 2015 as doi:10.1130/G36467.1

Geology

Global increase in plant carbon isotope fractionation following the Last Glacial Maximum caused by increase in atmospheric pCO_2

Brian A. Schubert and A. Hope Jahren

Geology published online 19 March 2015;
doi: 10.1130/G36467.1

Notes